

Kinetic Studies as a Method to Differentiate between Oxygen Species Involved in the Oxidation of Propene

Jerzy Haber^{*.1} and Wincenty Turek[†]

^{*}*Institute of Catalysis and Surface Chemistry, Polish Academy of Sciences, Krakow, Poland; and* [†]*Department of Physical Chemistry and Technology of Polymers, Silesian Technical University, Gliwice, Poland*

Received July 26, 1999; revised November 16, 1999; accepted November 19, 1999

Kinetic equations of propene oxidation along the nondestructive (nucleophilic oxidation to allylic products) and the destructive (electrophilic oxidation to degraded oxygenated and total oxidation products) pathways have been determined for three types of oxide catalysts: Bi₂O₃/MoO₃, giving only allylic products, Co₃O₄, showing only total oxidation, and SnO₂/MoO₃, giving both types of products. In all cases the reaction order of the nucleophilic oxidation was 1 with respect to propene and 0 with respect to oxygen, whereas that of electrophilic oxidation was close to 1 with respect to oxygen. The model of surface interactions is discussed in which propene reacts either with surface lattice oxide ions to give nucleophilic oxidation products or with transient surface oxygen species to give electrophilic oxidation. These transients result from the dynamic equilibrium between nonstoichiometric transition metal oxides and gas phase oxygen, so that the two kinetic equations are coupled by the equation expressing the equilibrium of surface oxygen vacancies. The rate constants of the homomolecular isotopic exchange of oxygen may be taken as a measure of the surface concentration of the transient oxygen species. © 2000 Academic Press

INTRODUCTION

Interaction of a hydrocarbon molecule with oxygen at the surface of an oxide catalyst results in a network of parallel and consecutive elementary steps, in which hydrogen is abstracted, nucleophilic oxygen is inserted, electrophilic oxygen reacts with π -electrons, and C–C bonds are cleaved (1–3). For the catalyst to be selective, it must accelerate those consecutive steps which lead to the desired product and depress all others. In the case of olefins, in the heterogeneous oxidation by gas phase oxygen on oxide catalysts, abstraction followed by the nucleophilic addition of lattice oxygen results in the selective allylic oxidation, whereas interaction with the electrophilic oxygen leads to the cleavage of the C=C bond, to the formation of oxygenated alkane

¹ To whom correspondence should be addressed. Institute of Catalysis and Surface Chemistry, Polish Academy of Sciences, Ul. Niezapominajek, 30-239 Kraków, Poland. Fax: +48 12 425 19 23. E-mail: nchaber@cyf.kr.edu.pl.

derivatives, and finally to total oxidation (4–6). It can be expected that the rates of these two reaction pathways would follow different kinetic equations and that it should be possible to discriminate between these two processes on the basis of kinetic studies. Unfortunately, in the literature only the kinetic equations describing the overall reaction rate are available, which do not permit conclusions to be drawn about the contribution of different pathways. Thus, it seemed interesting to determine the rate equations of different elementary steps in the selective and the total oxidation, to discriminate between the participation of different oxygen species and elucidate the reaction mechanism.

The reaction orders of the oxidation of propene to different products of the selective and the total oxidation have been determined. Three catalysts were used for the kinetic studies, carried out in the temperature range 600–700 K: Bi₂O₃/MoO₃, which is known to give acrolein as the product of the allylic oxidation with very high selectivity, Co₃O₄, which is known as the total oxidation catalyst, and SnO₂/MoO₃, which gives products of both selective and total oxidation.

EXPERIMENTAL

Determination of Catalytic Activity

The tests of the kinetics of propene oxidation were performed in a glass reactor with an inside diameter of 18 mm (7). The kinetics measurements were carried out using the differential method. The propene conversion degree was 5–15%. Samples of the catalyst of ≈ 3 g each and with grain diameters up to 0.75 mm were used. The catalyst bed height in the reactor was lower than its diameter in all cases. The reagents, propene and oxygen, were diluted with nitrogen to ensure their appropriate concentrations in the reaction mixture. A constant flow rate of the reaction mixture was maintained throughout the entire experiment at the value of 15.0 dm³/h.

The reaction products were analysed by gas chromatography. Organic compounds were separated in a steel column of 3-mm diameter and 3-m length, packed with 4%

of Carbowax 20 M on Chromosorb G, AW, DMCS, 80/100 mesh, and detected by FID; CO and CO₂ were separated in a steel column of 3-mm diameter and 2-m length, packed with activated charcoal, 60/80 mesh, and detected by TCD.

Kinetics of the reaction is usually determined using the Ostwald method with one of the reagents being taken in a very high excess. In such conditions, however, a different reaction mechanism may occur as compared to the reaction mixture, containing both reagents in comparable concentrations. This may affect also the form of the kinetic equation obtained. Therefore, in the present study, the measurements were carried out in such a way that comparable reagent concentrations (the ratio of concentrations of oxygen to propene was kept within the limits 0.78–2.83) were used when determining the reaction orders. From the values of the rates of formation of different products, the order with respect to propene and oxygen has been determined separately for the reaction of the allylic (nucleophilic) oxidation and the destructive (electrophilic) oxidation.

In the case of MoO₃-based catalysts, measurements were carried out at constant temperature in two series: (I) at constant oxygen concentration with varying propene concentration and (II) at constant propene concentration with varying oxygen concentration.

In the determination of the reaction order of propene oxidation over Co₃O₄, the difficulty arose in ensuring a constant temperature on varying the gas phase composition due to the high exothermicity when propene was oxidized mainly to CO₂. Therefore, a method had to be used in which the temperature dependence of the reaction rate was determined for three different oxygen : propene molar ratios from which reaction orders with respect to propene and oxygen at a selected temperature could be calculated. Such an approach was adopted because even in the case of a strongly exothermic reaction it permits measurements of kinetics to be performed with high precision at several freely chosen and easily measurable temperatures.

Materials

The Bi₂O₃/MoO₃ and SnO₂/MoO₃ catalysts were obtained by the impregnation of MoO₃, supplied by Cli-

max Molybdenum Co. (surface area determined by the BET method from low-temperature krypton adsorption was 2.59 m²/g), with Bi³⁺ and Sn⁴⁺ ions from the appropriate nitrate solutions. As indicated by the XPS analysis (8), the Bi³⁺ ions are located at the surface of MoO₃ crystallites. The concentrations of depositing ions were chosen so that the solution, taken to prepare the slurry, contained the amount of metal ions required to produce the surface coverage of MoO₃ of 1 monolayer and to obtain 1.0Bi₂O₃/MoO₃ and 1.0SnO₂/MoO₃. The slurry was first slowly dried at room temperature with continuous stirring and then dried at 413 K for 10 h. Finally, the samples were calcinated at 773 K for 5 h in air. Co₃O₄ was obtained as the result of decomposition of Co(OH)₂, carried at 833 K for 6 h in air. Cobalt hydroxide was obtained through precipitation from the cobalt nitrate solution by sodium hydroxide.

RESULTS

(1) Bi₂O₃/MoO₃ Catalyst

Selectivities of propene oxidation over the investigated catalysts are compared in the Table 1.

Oxidation of propene over the 1.0Bi₂O₃/MoO₃ catalyst at 617 K resulted in the formation of acrolein with a selectivity of 97.2% at conversion ranging from 5 to 15%. The only other detectable product was acetaldehyde formed with a selectivity of 2.8%. The total oxidation to CO₂ was negligible.

Figure 1 shows the results of the determination of the propene oxidation rate at 617 K at constant oxygen concentration in the steady state, amounting to $x_{O_2} = 0.0232$ mole fraction as a function of propene concentration and Fig. 2 shows the results of the determination of the rate of propene oxidation at constant propene concentration in the steady state, amounting to $x_{pr} = 0.0188$ as a function of the concentration of oxygen. In all cases the concentrations of the reagents given on the abscissa were expressed by molar fractions and taken as arithmetic average values at the inlet and outlet of the reactor. On the basis of the $\log r = f(\log x_{pr})$ relationship, shown in Fig. 1, the reaction order of the oxidation of propene to acrolein with respect to propene was calculated to be $\beta_1 = 1$, while using the relationship $\log r = f(\log x_{O_2})$, shown in Fig. 2, the order of this reaction

TABLE 1
Selectivity of Propene Oxidation

Catalyst	Temp. (K)	Selectivity (%)					Total oxidation
		Acrolein	Acetic aldehyde	Ethyl acetate	Acrylic acid	Acetic acid	
1.0Bi ₂ O ₃ /MoO ₃	617	97.2	2.8	—	—	—	—
Co ₃ O ₄	521	0.2	0.4	—	—	—	99.4
1.0SnO ₂ /MoO ₃	624	31.1	5.2	1.6	2.2	3.9	56.0

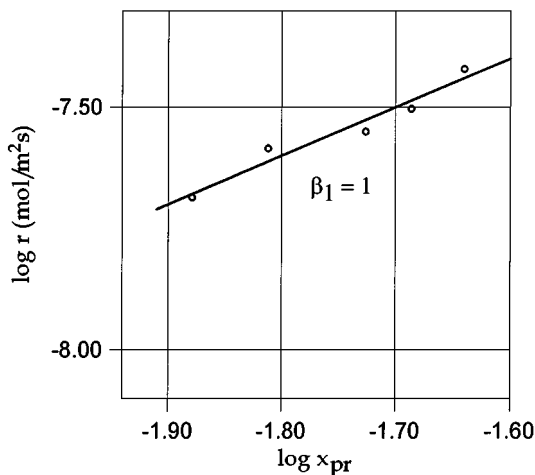


FIG. 1. The rate of oxidation of propene to acrolein over $1.0\text{Bi}_2\text{O}_3/\text{MoO}_3$ at 617 K as a function of the propene mole fraction x_{pr} , at a constant oxygen mole fraction, $x_{\text{O}_2} = 0.0232$. Order of reaction with respect to propene is $\beta_1 = 1$.

with respect to oxygen was calculated to be $\beta_2 = 0$. As oxidation of propene on this catalyst occurs virtually along the nondestructive, nucleophilic pathway with the selectivity to acrolein higher than 97%, it can be assumed that the reaction orders with respect to propene and oxygen, which have been determined, represent the orders of the nucleophilic propene oxidation pathway. The kinetics along this reaction pathway may thus be described by the following equation:

$$r = k \cdot p_{\text{C}_3\text{H}_6}. \quad [1]$$

(2) Co_3O_4 Catalyst

As already mentioned, the temperature dependence of the reaction rate was determined for different oxy-

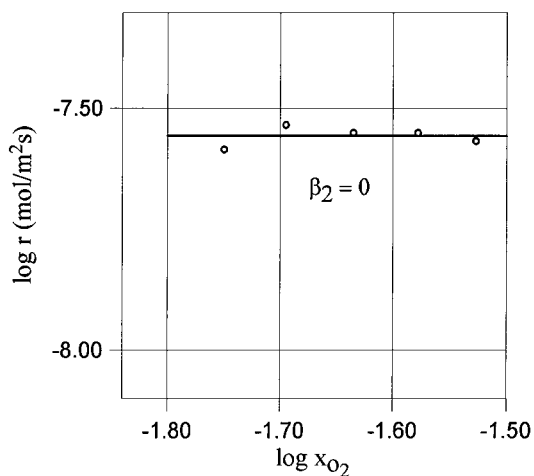


FIG. 2. The rate of oxidation of propene to acrolein over $1.0\text{Bi}_2\text{O}_3/\text{MoO}_3$ at 617 K as a function of the oxygen mole fraction x_{O_2} , at a constant propene mole fraction, $x_{\text{pr}} = 0.0188$. Order of reaction with respect to oxygen is $\beta_2 = 0$.

gen:propene molar ratios. The logarithm of the rate was plotted as a function of the reciprocal temperature. Parallel straight lines obtained indicated that the Arrhenius relationship is well obeyed, and the activation energy, and hence the reaction mechanism, does not change when the composition of the reaction mixture is changed. From these data the dependence of the reaction rate on the concentration of propene at a constant concentration of oxygen, and the dependence of the rate on the concentration of oxygen at a constant concentration of propene, could be obtained for any selected temperature and the reaction orders calculated. In the first series of measurements, performed at a constant starting concentration of oxygen, $x_{\text{O}_2} = 0.0280$ (mole fraction), in the reagents mixture, three various starting propene concentrations (in mole fractions) were used: $x_{\text{pr}} = 0.0178, 0.0140$, and 0.0099 . In the second measurement series, performed at a constant propene concentration, $x_{\text{pr}} = 0.0140$ (mole fraction), in the reagents mixture, three various starting oxygen concentrations were used: $x_{\text{O}_2} = 0.0347, 0.0280$, and 0.0214 . The reaction rates for each constant starting composition of reagents were measured at several temperatures, ranging from 495 to 524 K. The results obtained for mixtures with varying starting concentrations of propene and constant oxygen concentration are shown in Fig. 3, and those for varying starting concentrations of oxygen and constant propene concentration are shown in Fig. 4. The linear relationships of the function $\log r = f(1/T)$ shown in Figs. 3 and 4 are indicative of the reaction occurring in the kinetic range. The calculations of the reaction orders with respect to propene β_1 and with respect to oxygen β_2 were performed taking into account the reaction rates as read from the diagrams, for a selected temperature of 513 K ($10^3/T = 1.95$), the same for both series of measurements. The mean values were $\beta_1 = 0.71$ and $\beta_2 = 0.90$. The kinetics of the reaction of the total oxidation

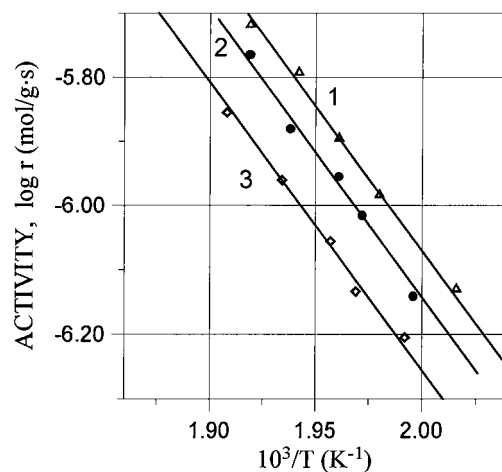


FIG. 3. The kinetics of complete propene oxidation over the Co_3O_4 catalyst at a constant oxygen concentration, $x_{\text{O}_2} = 0.0280$ (mole fraction) in the substrate mixture and at three different propene concentrations: (1) $x_{\text{pr}} = 0.0178$; (2) $x_{\text{pr}} = 0.0140$; (3) $x_{\text{pr}} = 0.0099$.

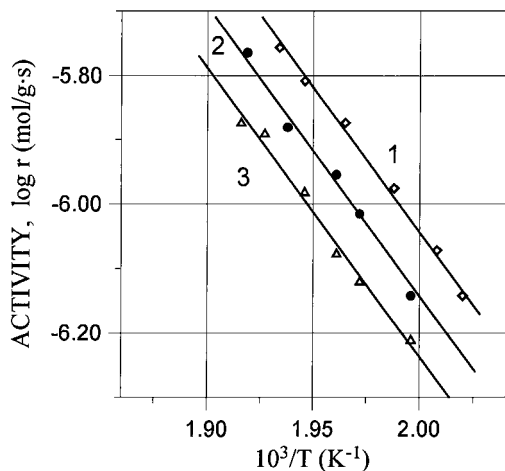


FIG. 4. The kinetics of complete propene oxidation over the Co_3O_4 catalyst at a constant propene concentration, $x_{\text{pr}} = 0.0140$ (mole fraction) in the substrate mixture and at three different oxygen concentrations: (1) $x_{\text{O}_2} = 0.0347$; (2) $x_{\text{O}_2} = 0.0280$; (3) $x_{\text{O}_2} = 0.0214$.

of propene (electrophilic oxidation), as determined for the Co_3O_4 catalyst, can thus be described by the equation

$$r = k \cdot p_{\text{C}_3\text{H}_6}^{0.71} \cdot p_{\text{O}_2}^{0.90} \quad [2]$$

(3) $\text{SnO}_2/\text{MoO}_3$ Catalyst

Measurements of the reaction rate over $\text{SnO}_2/\text{MoO}_3$ were carried out at 624 K. The results of the determinations of the oxidation rate at a constant oxygen concentration in the steady state, equal to $x_{\text{O}_2} = 0.0205$ molar ratio, as a function of the concentration of propene are plotted in Fig. 5, whereas the results obtained at constant propene concentration in the steady state, amounting to $x_{\text{pr}} = 0.0188$ molar

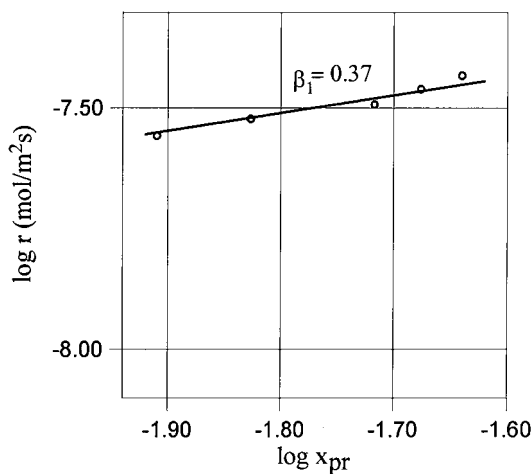


FIG. 5. The rate of propene reaction over the $1.0\text{SnO}_2/\text{MoO}_3$ catalyst at 624 K as a function of the propene mole fraction x_{pr} , at a constant oxygen mole fraction, $x_{\text{O}_2} = 0.0205$. Order of reaction with respect to propene is $\beta_1 = 0.37$.

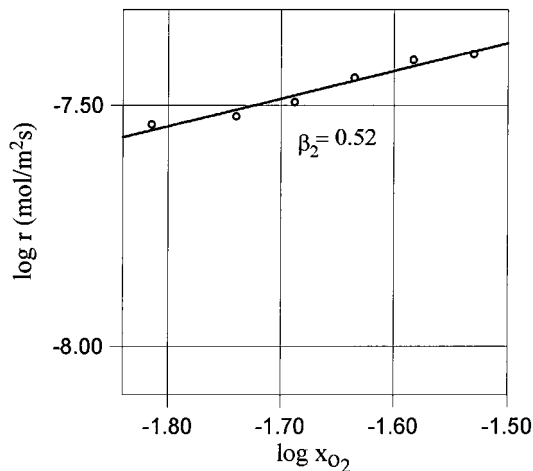
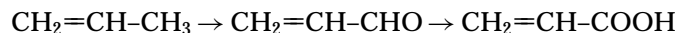


FIG. 6. The rate of propene reaction over the $1.0\text{SnO}_2/\text{MoO}_3$ catalyst at 624 K as a function of the oxygen mole fraction x_{O_2} , at a constant propene mole fraction, $x_{\text{pr}} = 0.0192$. Order of reaction with respect to oxygen is $\beta_2 = 0.52$.

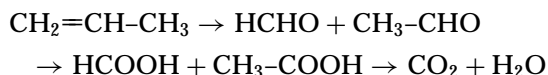
ratio, as a function of oxygen concentration, are plotted in Fig. 6. On the basis of these results the orders of the overall reaction of propene oxidation with respect to propene and oxygen were calculated to be $\beta_1 = 0.37$ and $\beta_2 = 0.52$, respectively. Kinetics of the overall reaction of propene oxidation on the surface of the $\text{SnO}_2/\text{MoO}_3$ catalyst may thus be described by the formula

$$r = k \cdot p_{\text{C}_3\text{H}_6}^{0.37} \cdot p_{\text{O}_2}^{0.52} \quad [3]$$

Then, for the same catalyst, the rates of oxidation of propene to the products of the nondestructive oxidation (nucleophilic oxidation)



and the products of the destructive oxidation (electrophilic oxidation)



obtained at constant oxygen pressure were plotted separately as a function of propene concentration x_{pr} (Fig. 7). The calculated reaction orders with respect to propene amounted to $\beta_1^{\text{sel}} = 0.86$ and $\beta_1^{\text{tot}} = 0.24$ for nucleophilic and electrophilic oxidation, respectively. Similarly, these rates obtained at constant propene pressure were plotted separately as a function of oxygen concentration, x_{O_2} (Fig. 8). The calculated reaction orders with respect to oxygen amounted to $\beta_2^{\text{sel}} = 0.07$ and $\beta_2^{\text{tot}} = 0.87$, respectively. Kinetics of the oxidation of propene along the two reaction pathways is thus described by two different formulas:

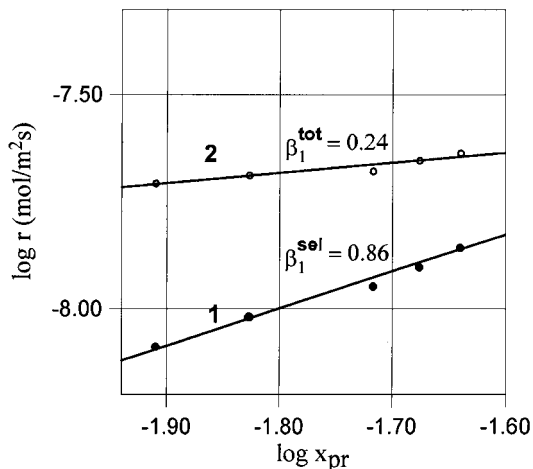


FIG. 7. The rate of propene reaction over the $1.0\text{SnO}_2/\text{MoO}_3$ catalyst at 624 K as a function of the propene mole fraction x_{pr} , at a constant oxygen mole fraction, $x_{\text{O}_2} = 0.0205$. (1) Rate of the reaction leading to the products of the nondestructive oxidation; (2) rate of the destructive oxidation reactions. The orders of reaction with respect to propene in these reactions are $\beta_1^{\text{sel}} = 0.86$ and $\beta_1^{\text{tot}} = 0.24$, respectively.

the nondestructive (nucleophilic) oxidation,

$$r_{\text{sel}} = k_{\text{sel}} \cdot p_{\text{C}_3\text{H}_6}^{0.86} \cdot p_{\text{O}_2}^{0.07}; \quad [4]$$

the total (electrophilic) oxidation,

$$r_{\text{tot}} = k_{\text{tot}} \cdot p_{\text{C}_3\text{H}_6}^{0.24} \cdot p_{\text{O}_2}^{0.87}. \quad [5]$$

It can be noticed that within the limits of experimental error the kinetics of propene oxidation along the selective oxidation pathway is described by a rate equation (Eq. [4]) similar to the case of highly selective oxidation catalyst

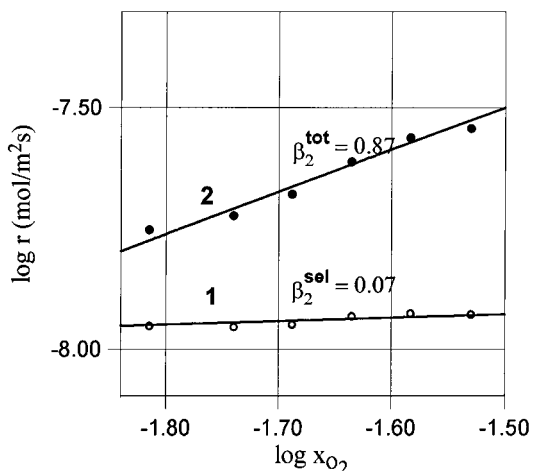


FIG. 8. The rate of propene reaction over the $1.0\text{SnO}_2/\text{MoO}_3$ catalyst at 624 K as a function of the oxygen mole fraction x_{O_2} , at a constant propene mole fraction, $x_{\text{pr}} = 0.0192$. (1) Rate of the reaction leading to the products of the nondestructive oxidation; (2) rate of the destructive oxidation reactions. The orders of reaction with respect to oxygen in these reactions are $\beta_2^{\text{sel}} = 0.07$ and $\beta_2^{\text{tot}} = 0.87$, respectively.

$\text{Bi}_2\text{O}_3/\text{MoO}_3$ (Eq. [1]), whereas the reaction along the total oxidation pathway (Eq. [5]) has the order, with respect to oxygen, similar to the total oxidation observed on the Co_3O_4 catalyst.

DISCUSSION

Transition metal oxides are nonstoichiometric compounds, with the composition depending on the equilibrium between the lattice and its constituents in the gas phase. In the equilibrium state, the chemical potential of oxygen in the gas phase is equal to the chemical potential of oxide ions in the lattice:

$$\mu_{\text{O}_2} = \mu_{\text{O}^{2-}}. \quad [6]$$

Chemical potential of oxygen in the gas phase may be expressed as a function of its pressure,

$$\mu_{\text{O}_2} = \mu_{\text{O}_2}^0 + RT \ln p_{\text{O}_2}; \quad [7]$$

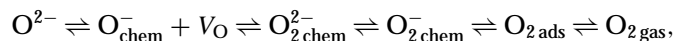
from Eqs. [6] and [7] it follows that the chemical potential of lattice oxide ions is also a function of oxygen pressure,

$$\mu_{\text{O}^{2-}} = \mu_{\text{O}^{2-}}^0 + RT \ln p_{\text{O}_2}. \quad [8]$$

Changes of the chemical potential of oxide ions in the crystal lattice are effected by the generation of lattice defects, which results in the changes of stoichiometry of the oxide. Hence, the nonstoichiometry is a function of oxygen pressure:

$$(\text{metal} : \text{oxygen})_{\text{oxide}} = f(p_{\text{O}_2}).$$

The equilibrium between the oxide lattice and the gas phase is a dynamic equilibrium, in which the rate of dissociation of the oxide lattice and evolution of oxygen in the form of O_2 gas is equal to the rate of its incorporation from the gas phase. In the process of dissociation the oxide ions must be extracted from the surface, electrons injected into the solid, oxygen atoms recombine to form molecules, and desorb as dioxygen. The reverse series of elementary steps must take place upon incorporation. These elementary steps result in surface equilibria,



so that the surface is always covered by different oxygen species, as illustrated in Fig. 9. The surface coverage by these species depends on the oxygen pressure in the gas phase, the rate constants of adsorption and chemisorption (transfer of electrons between adsorbed oxygen molecules and the solid), the rate of incorporation, and the dissociation pressure of the oxide. At low temperatures only the surface layer of the oxide may be equilibrated with the gas phase; at sufficiently high temperatures the defects created at the surface diffuse into the bulk and equilibrium is established between

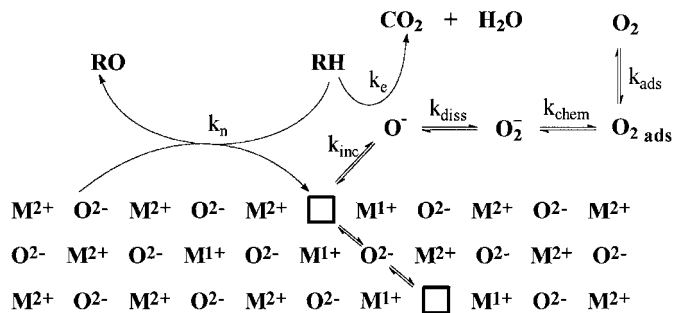
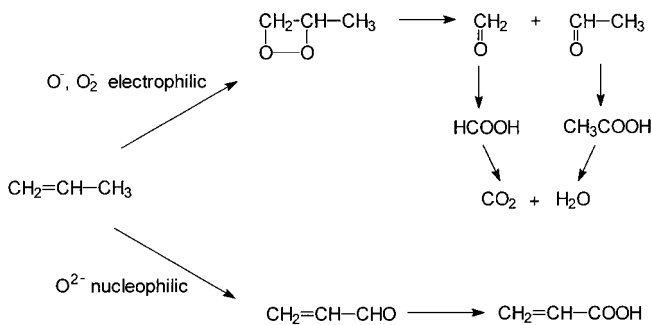


FIG. 9. The mechanism of the olefins oxidation reaction over oxide catalysts.

the gas phase and the solid oxide. O^{2-} ions, exposed at the surface, are nucleophilic reagents, whereas $O_{2\text{chem}}^-$, O_{chem}^- , and $O_{2\text{ads}}$ are electrophilic species. When such a surface is contacted with propene molecules, electrophilic oxygen species attack the π -bond of propene to form epoxy or peroxy complexes, which react further by cleavage of the C-C bonds and form acetaldehyde, formaldehyde, the corresponding acids, esters, and CO_2 (scheme 1). In the parallel reaction pathway, nucleophilic oxide ions O^{2-} react with activated propene molecules to form acrolein (for simplicity we shall consider only the overall reaction of the oxidation of propene to acrolein and acrylic acid).

Thus, different oxygen species, present at the oxide surface, compete for propene molecules. Moreover, a competition also exists between propene molecules and surface oxide vacancies for the electrophilic O_{chem}^- species, which can either be captured by propene to form products of electrophilic oxidation ($\text{CO}_2 + \text{H}_2\text{O}$ in Fig. 9) or be incorporated into the surface by reaction with oxygen vacancies V_{O} . The rate of the reaction along the nucleophilic oxidation pathway is proportional to the pressure of propene and the number of lattice oxide ions exposed at the surface. The latter is equal to the total number of lattice anionic surface sites, which is constant, minus the surface concentration of vacancies, which can be expressed by the degree of reduction α . Hence, the rate of nucleophilic oxidation is given by



SCHEME 1

the equation

$$r_n = k_n \cdot p_{\text{C}_3\text{H}_6} (1 - \alpha). \quad [9]$$

When the reaction is carried out in an excess of oxygen in the gas phase, the catalyst surface is fully oxidized, $\alpha = 0$, and the rate of the reaction is expressed by the formula

$$r_n = k_n \cdot p_{\text{C}_3\text{H}_6}. \quad [10]$$

This equation describes well not only the reaction at the surface of the $\text{Bi}_2\text{O}_3/\text{MoO}_3$ catalyst, where only nucleophilic oxidation takes place but also the reaction along the nucleophilic oxidation pathway in the case of the $\text{SnO}_2/\text{MoO}_3$ catalyst, when electrophilic oxidation is competing in a parallel pathway.

In the case of the electrophilic oxidation pathway the rate of the reaction is proportional to propene pressure and to surface coverage with electrophilic oxygen species O_{chem}^- , $O_{2\text{chem}}^-$, and $O_{2\text{ads}}$:

$$r_e = k_e \cdot p_{\text{C}_3\text{H}_6} \cdot \theta_{\text{O}}. \quad [11]$$

The surface coverage with electrophilic oxygen in the stationary state of the reaction is the result of its supply by adsorption and its removal through the reaction with propene molecules and the competing incorporation into the surface vacancies,

$$k_{\text{ads}} \cdot p_{\text{O}_2} = k_{\text{inc}} \cdot \alpha \cdot \theta_{\text{O}} + k_e \cdot p_{\text{C}_3\text{H}_6} \cdot \theta_{\text{O}}, \quad [12]$$

and

$$\theta_{\text{O}} = \frac{k_{\text{ads}} \cdot p_{\text{O}_2}}{k_{\text{inc}} \cdot \alpha + k_e \cdot p_{\text{C}_3\text{H}_6}}. \quad [13]$$

The rate of electrophilic oxidation can thus be expressed by the equation

$$r_e = \frac{k_e \cdot k_{\text{ads}} \cdot p_{\text{C}_3\text{H}_6} \cdot p_{\text{O}_2}}{k_{\text{inc}} \cdot \alpha + k_e \cdot p_{\text{C}_3\text{H}_6}}. \quad [14]$$

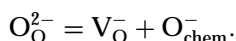
The reaction should be of the first order with respect to oxygen, which has indeed been observed in the case of the total oxidation catalyst Co_3O_4 and has also been found to hold along the electrophilic oxidation pathway in the case of the $\text{SnO}_2/\text{MoO}_3$ catalyst. The fractional order with respect to propene depends on the relative importance of the incorporation of oxygen into surface vacancies as compared to its reaction with propene.

It may thus be concluded that two parallel reaction pathways may be followed by propene when adsorbed at the surface of an oxide catalyst: its selective allylic oxidation by surface lattice oxide ions (nucleophilic oxidation) and its destructive oxidation by reactive oxygen species O_{chem}^- , $O_{2\text{chem}}^-$, and $O_{2\text{ads}}$ (electrophilic oxidation). These two reaction pathways are described by different rate equations, but are coupled together by the equation, describing

TABLE 2
Homomolecular Isotopic Exchange of Oxygen

Oxide	Temperature range (K)	Rate of reaction (mol cm ⁻² s ⁻¹)	Activation energy (kJ mol ⁻¹)	References
Bi ₂ O ₃ ·MoO ₃ (1:1)	747-773	No exchange		(9), (10), (11)
MoO ₃	798-873	1.0 × 10 ⁵	213	(12)
SnO ₂	723-793	4.0 × 10 ⁸	113	(12)
Co ₃ O ₄	398-523	2.0 × 10 ¹³	67	(12)

the generation and annihilation of surface oxygen vacancies:



The importance of these two pathways depends on the relative values of k_n , k_e , k_{inc} , k_{diss} , k_{chem} , and k_{ads} . The first two rate constants depend on the nature of the hydrocarbon molecule, whereas the rate constants describing the transformations of surface oxygen species k_{inc} , k_{diss} , k_{chem} , and k_{ads} are characteristic of the oxide. No data exist which would enable the separate calculation of their values; one can, however, assume that measurements of the rate of homomolecular isotopic exchange of oxygen could permit the comparison of these values for different oxides. The rate constants of the homomolecular isotopic oxygen exchange for the oxides studied, as taken from Refs. (9-12), are summarized in Table 2. The highest rate of exchange is observed on the surface of Co₃O₄, which indicates that the surface of this oxide shows the highest coverage with electrophilic oxygen species. Accordingly, only the electrophilic oxidation, mainly to the total combustion products, is found. Practically, no exchange is observed in the case of Bi₂O₃/MoO₃. Thus, no chemisorbed electrophilic oxygen species are present at the surface, only oxide ions, and the selectivity to allylic oxidation products (nucleophilic oxidation) is very high. The rate of exchange at the surface of SnO₂ is 5 orders of magnitude smaller than that at the surface of Co₃O₄, but many orders of magnitude greater than that in the case of the Bi₂O₃-MoO₃ system. Thus, the surface is much less populated with electrophilic oxygen species and both—the electrophilic and the nucleophilic oxidation pathways—are followed in similar proportions. The present study leads to the conclusion that the two pathways are described by different rate equations and can be identified by the kinetic measurements.

CONCLUSION

At the surface of oxide catalysts propene is oxidized along two parallel reaction pathways in which two different types of oxygen take part: one characteristic for the selective oxidation catalysts, which has been identified earlier as the lattice oxygen (9), and the second, characteristic of the total oxidation catalysts, appearing at the surface as the result of the dynamic equilibrium between the metal oxide and the gas phase oxygen. The two pathways are described by different rate equations and can be identified by kinetics measurements.

REFERENCES

1. Bielanski, A., and Haber, J., "Oxygen in Catalysis." Marcel Dekker Inc., New York, 1991.
2. Haber, J., "Studies Surface Science Catalysis," Vol. 72, p. 279. Elsevier, Amsterdam, 1992.
3. Grasselli, R. K., and Burrington, J. D., *Adv. Catal.* **30**, 133 (1981).
4. Libre, J. M., Barbaux, Y., Grzybowska, B., and Bonnelle, J. P., *React. Kinet. Catal. Lett.* **20**, 249 (1982).
5. Haber, J., "Proceedings Symposium Heterogeneous Hydrocarbon Oxidation" (B. K. Warren, and S. Ted. Oyama, Eds.), ACS Symposium Series 638, p. 20. American Chemical Society, Washington D.C., 1996.
6. Haber, J., *Studies Surface Science Catalysis*, Vol. 110, p. 1. Elsevier, Amsterdam, 1997.
7. Brückman, K., Haber, J., and Turek, W., *J. Catal.* **114**, 169 (1988).
8. Brückman, K., Haber, J., and Wiltowski, T., *J. Catal.* **106**, 188 (1987).
9. Keulks, G. W., Krenzke, L. D., and Noterman, T. M., *Adv. Catal.* **27**, 183 (1978).
10. Keulks, G. W., *J. Catal.* **19**, 232 (1970).
11. Wragg, R. D., Ashmore, P. G., and Hockey, J. A., *J. Catal.* **22**, 49 (1971).
12. Borekov, G. K., "Catalysis: Science and Technology," Vol. 3, p. 39. Springer Verlag, Berlin, 1982.